



Synthesis and Th1-immunostimulatory activity of α -galactosylceramide analogues bearing a halogen-containing or selenium-containing acyl chain



Md. Imran Hossain^{a,b}, Shinya Hanashima^{a,*}, Takuto Nomura^a, Sébastien Lethu^b, Hiroshi Tsuchikawa^a, Michio Murata^{a,b,*}, Hiroki Kusaka^c, Shunsuke Kita^c, Katsumi Maenaka^c

^a Department of Chemistry, Graduate School of Science, Osaka University, 1-1 Machikaneyama, Toyonaka, Osaka 560-0043, Japan

^b JST, ERATO, Lipid Active Structure Project, Osaka University, 1-1 Machikaneyama, Toyonaka, Osaka 560-0043, Japan

^c Laboratory of Biomolecular Science, Faculty of Pharmaceutical Sciences, Hokkaido University, Sapporo 060-0812, Japan

ARTICLE INFO

Article history:

Received 9 May 2016

Revised 3 June 2016

Accepted 3 June 2016

Available online 6 June 2016

Keywords:

α -GalCer

Cytokines

CD1d

Natural product synthesis

Glycosylation

ABSTRACT

A novel series of CD1d ligand α -galactosylceramides (α -GalCers) were synthesized by incorporation of the heavy atoms Br and Se in the acyl chain backbone of α -galactosyl-*N*-cerotoylphosphingosine. The synthetic analogues are potent CD1d ligands and stimulate mouse invariant natural killer T (iNKT) cells to selectively enhance Th1 cytokine production. These synthetic analogues would be efficient X-ray crystallographic probes to disclose precise atomic positions of alkyl carbons and lipid–protein interactions in KRN7000/CD1d complexes.

© 2016 Elsevier Ltd. All rights reserved.

1. Introduction

Marine invertebrates are a rich source of pharmacologically active compounds. Agelasphins are a class of such natural products, isolated from the Okinawan marine sponge *Agelas mauritanicus*.^{1,2} These glycosphingolipids show potent in vivo antitumor activity through stimulation of the host immune system. The structural optimizations of the agelasphins have led to the development of a very potent immunostimulatory agent, KRN7000 (Fig. 1),³ which is a simple α -galactosylceramide (α -GalCer). The innate receptor of KRN7000 has been identified as the antigen presentation protein CD1d.^{4,5} The α -GalCer–protein complex is further recognized by T-cell receptors (TCRs) expressed on invariant natural killer T cells (iNKT). The structure of this CD1d/ α -GalCer/TCR ternary complex has been established by X-ray crystallography.^{6,7} However, the atomistic mechanism of ligand recognition by CD1d remains elusive mainly due to ambiguity in the X-ray crystal structures; the dispersed electron density of a bound α -GalCer impeded the precise elucidation of the alkyl-chain conformation in the deep binding pockets of CD1d (Fig. 2). We have recently

disclosed that a simple alkyl chain of lipids sometimes plays a crucial role in ligand–receptor interactions using an ultra-high resolution protein–ligand complex (0.86–0.93 Å).^{8,9} However, with the large CD1d/KRN7000/TCR complex, it would not be easy to prepare high quality crystals necessary for high resolution density maps. To address this issue, we designed α -GalCer probes, **3**, **4**, and **5**, which possess an electron-rich heavy atom (Br or Se) in the acyl chain (Fig. 1). Br or Se is incorporated in **3**, **4**, and **5** by substituting a C₁ segment at C12', C18', or C26', respectively (Fig. 2). These positions are expected to act as milestones to determine the shape of the acyl chain by X-ray crystallography, because the heavy atoms are positioned at the beginning (C12') and middle (C18') of the loop, and at the terminus (C26') of the chain.

The bromine substituent was employed because Br and a methyl group have similar van der Waals radii (Br: 185 pm; CH₃: 200 pm). The selenoether group was adopted in the place of the methylene C12' or C18' because of the similar bond angles (C–Se–C: 96.3°; C–C–C 112.6°) and van der Waals radii (Se: 190 pm; CH₂: 200 pm), but it does have a slightly larger bond length (C–Se: 194.5 pm; C–C: 154.0 pm). More importantly, the distance between the two carbon atoms of a C–Se–C moiety is 289.8 pm, which is a little larger than the distance of 1,3-carbon atoms in alkane by 34 pm, but should not significantly affect the conformation of the whole acyl chain except for the selenoether

* Corresponding authors. Tel.: +81 6 6850 5789 (S.H.), +81 6 6850 5774 (M.M.).

E-mail addresses: hanashimas13@chem.sci.osaka-u.ac.jp (S. Hanashima), murata@chem.sci.osaka-u.ac.jp (M. Murata).

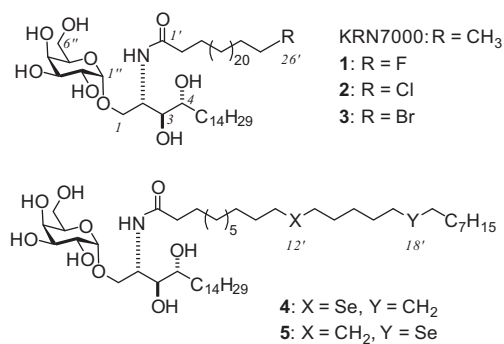


Figure 1. Structures of KRN7000 and its analogues 1–5 with a halogen or selenium atom.

and its neighboring portions. Such heavy atoms at α -GalCer probes are also expected to play a key role in phase determination in X-ray crystallography by using the anomalous dispersions in single- or multi-wavelength anomalous dispersion (SAD or MAD) methods.¹⁰ The selenoether moiety has been used previously as an analogue of oxygen and sulfur atoms in protein ligands or in target proteins, and selenoglycoside ligands including KRN7000 have been synthesized^{11,12} to determine phasing of the protein crystals.¹³ On the other hand, no X-ray crystallographic analysis has been reported for the selenoether moiety used as a substitute for a methylene segment.

The CD1d/ α -GalCer/TCR complex provides an ideal system to investigate molecular mechanisms underlying Th1/Th2 immunological switching, in which the TCR regulates a wide range of responses.^{14,15} Exogenous α -GalCer antigens bound to CD1d are presented to iNKT cells through TCRs at the cell surface, which leads to the activation of iNKT cells.¹⁶ The activate cells induce the production of cytokines such as interferon gamma (IFN- γ), interleukin (IL)-12, and granulocyte macrophage colony-stimulating factor (GM-CSF) of the Th1 immune pathway, and activation of cellular immunity for tumor rejection.^{17–19} This ternary complex also enhances the production of IL-4 and IL-13 that involve the Th2 pathway for humoral immunity.^{20,21} For this reason, a balance in the production of Th1 and Th2 cytokines is a key point for controlling the immune responses in various diseases,^{22–24} including cancer,^{18,25} diabetes,^{26–28} and infections; CD1d-restricted iNKT cells

are reported to inhibit the intrahepatic-stage infection of the rodent malaria parasites *Plasmodium berghei*,²⁹ and IFN- γ inhibits hepatitis B virus replication.³⁰ In addition, such CD1d-restricted iNKT cell ligands are generally known as potent vaccine adjuvant.³¹ Therefore, the CD1d ligands that can fine-tune the balance of Th1/Th2 cytokine secretion would be potential drug lead compounds.

The proportion of Th1/Th2 cytokine production is thought to depend on the stability of the CD1d/ α -GalCer/TCR complex.^{6,7,32} Stronger stimulation for a longer period is required for the Th1 pathway (IFN- γ production) while a weaker and shorter stimulation period results in stimulation of the Th2 pathway (IL-4 production).²¹ The X-ray crystal structure of the ternary complex has revealed that the phytosphingosyl and acyl chains are incorporated into the two deep hydrophobic binding pockets F' and A', respectively, and the 3-OH of phytosphingosine is involved in the hydrogen bonding to Asp80 on CD1d⁵ and Arg95 of the TCR.⁶ Furthermore, the α -galactoside moiety is directly presented to the TCR at the surface of CD1d. Hydroxy groups of the galactose, particularly 2''-, 3''-, and 4''-OH, interact with Gly96, Ser30, and Phe29 of the TCR.⁶

To improve the cytokine production activity and selectivity, various derivatives of KRN7000 have been synthesized.^{33–37} Notably, modifications of the alkyl chains in the sphingosine and fatty acyl moieties significantly influenced the balance of Th1/Th2 cytokine production. Truncation of the acyl chain (C8) leads to higher Th2 selectivity compared to full-length KRN7000.³⁸ A shorter acyl chain with a terminal hydroxy group or with the replacement of the amide moiety with a triazole group also enhances Th2 selectivity.^{39,40} Similarly, a shorter alkyl chain of the phytosphingosine chain elicits more Th2 responses.⁴¹ On the other hand, shortening and/or introduction of an aromatic group in the fatty acid chain (C8Ph) resulted in the highest Th1-biased cytokine production in human NKT cell lines; MD simulations revealed that the interaction between the phenyl group and the aromatic residues Tyr73 or Trp40 of CD1d could stabilize the ternary complex.^{42,43} Replacement of the anomeric oxygen atom by a methylene group enhances the selectivity toward Th1.³⁶ Most of the synthetic variants that show Th1/Th2 selectivity are modified at either the phytosphingosine or acyl chain of α -GalCer. As a consequence, these structural alterations in the ceramide portion relevant to its binding affinity to CD1d may allow us to fine-tune the stability of the ternary complex, which is thought to be a key factor for selective cytokine production. To determine the exact atomic positions of the acyl chain, we designed α -GalCer probes 3–5 (Fig. 1) preserving most of the hydrophobic interactions in the ligand–protein complex. Whether the Se or Br substitution influenced the binding to CD1d was evaluated through a cytokine (IFN- γ and IL-4) production assay. In addition, we were also interested in the effect of the electron negativity and possible halogen bond interactions at the terminal halogens. We therefore prepared F and Cl substituted derivatives 1 and 2 (Fig. 1). All of our synthetic α -GalCer probes successfully stimulated the production of Th1 and Th2 cytokines, suggesting their potential use for co-crystallization with CD1d to determine precise lipid–protein interactions by X-ray crystallography.

2. Results

2.1. Chemical synthesis

The halogenated fatty acids were synthesized from reported compounds **6**⁴⁴ and **9**⁴⁵ (Scheme 1). The hydroxy group of **6** was converted to *N*-phenyl-tetrazolyl-sulfide (**7**), which was oxidized to *N*-phenyl-tetrazolyl-sulfone (**8**). The benzyl hemiester **9** was reduced to give **10**, and the following oxidation yielded aldehyde

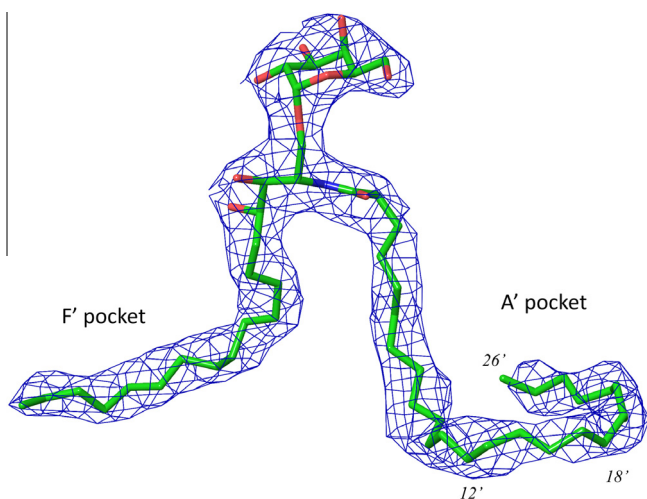
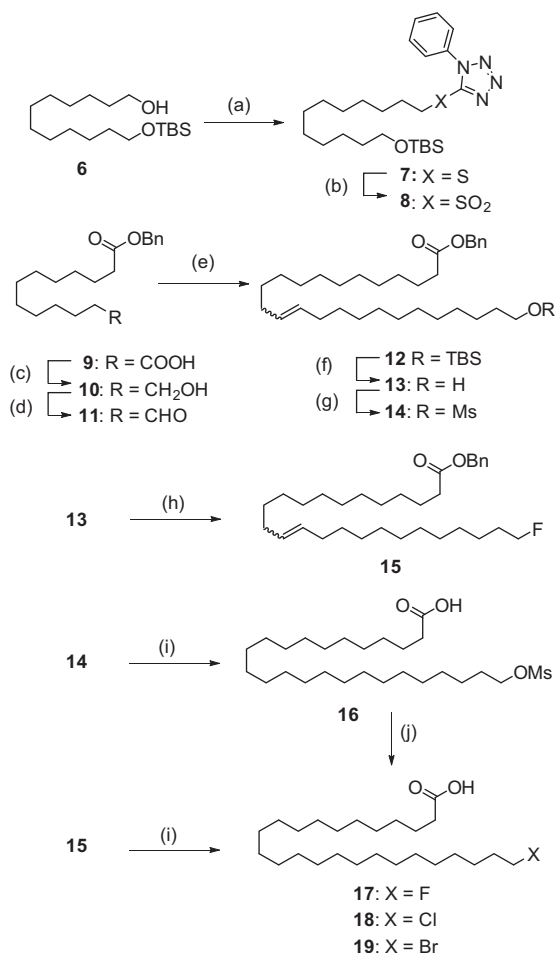


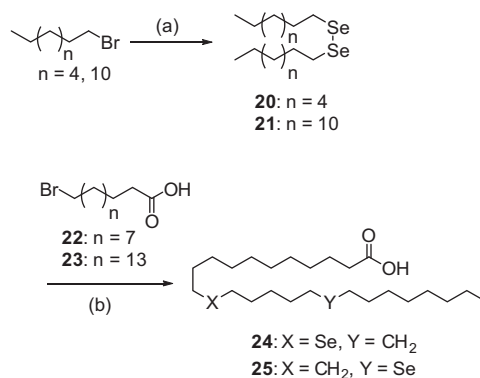
Figure 2. Electron density map of KRN7000 bound in human CD1d (PDB ID: 3HUJ). Blue mesh shows the density of 1.0 σ . The dispersed electron density prevents the determination of atomic positions precisely. In this study, the heavy atoms Se and Br are incorporated at C12' or C18', and at C26', respectively, to enhance the electron density of the labeled positions.



Scheme 1. Synthesis of halogenated fatty acids **17**, **18**, and **19**. Reagents and conditions: (a) 1-Phenyl-1H-tetrazole-5-thiol, Ph_3P , DEAD, THF, 96%; (b) *m*-CPBA, CH_2Cl_2 , 84%; (c) BH_3 -THF, THF, 0 °C to rt, 82%; (d) PCC, sodium acetate, CH_2Cl_2 , 80%; (e) **8**, LHMDS THF, -78 °C to rt, 80%; (f) TBAF, THF, 80%; (g) MsCl, pyridine, THF, 94%; (h) DAST, CH_2Cl_2 , 0 °C to rt, 40%; (i) $Pd(OH)_2 \cdot C$, Et_3SiH , MeOH/ CH_2Cl_2 = 3:5, 1 h **16**: 80%, **17**: 85% (j) KCl or KBr, $(Bu_4N)HSO_4$, H_2O , toluene, 100 °C, 4 h, **18**: 90%, **19**: 93%.

11. The Julia-Kocienski olefination reaction was applied to form alkene **12** (*E/Z* = 3:1) from the precursors **8** and **11**. The TBS protection of **12** was removed with TBAF to give **13**. The fluoropentacosanoic acid **17** was synthesized from the common intermediate **13** using the fluorinating agent diethylaminosulfur trifluoride (DAST) and the subsequent hydrogenation procedures. Chloro or bromo pentacosanoic acids **18** and **19** were synthesized by mesylation of **13** using MsCl, and the yielded compound **14** was treated with activated palladium hydroxide on carbon in the presence of Et_3SiH to yield the carboxylic acid **16**. Finally, heating of compound **16** with excess amount of KCl or KBr in biphasic medium (toluene/water) provided the desired chloro or bromo pentacosanoic acids **18** and **19**, respectively.

Selenocerotic acids **24**⁴⁶ and **25** were prepared in two steps (Scheme 2): first dialkyl diselenides (**20** and **21**) were synthesized from bromoalkanes and diselenide, the latter of which was prepared in situ from metallic selenium and sodium borohydride.⁴⁷ Bromoalkyl carboxylic acid (**23**) was synthesized according to the similar synthetic scheme shown in Scheme 1 (see Supporting information). The intermediates **20** and **21** thus obtained were next reduced by sodium borohydride again and reacted with bromoalkyl carboxylic acids (**22** and **23**) to yield selenocerotic acids **24** and **25**.^{48,49}



Scheme 2. Synthesis of selenocerotic acids **24** and **25**. Reagents and conditions: (a) Se, $NaBH_4$, EtOH, 62%; (b) $NaBH_4$, THF, H_2O , 42% for **24** and 42% for **25**.

To synthesize α -GalCer analogues, the key intermediate **29**⁵⁰ was prepared by glycosylation of donor **27** and acceptor **28** (Scheme 3). The protected galactose precursor (**26**) was obtained by a reported method.⁵¹ Treatment of **26** with DAST and NBS yielded a mixture of α,β -isomers (α/β = 4:1). The α -isomer **27** was separated for the use of the following reactions. The glycosyl acceptor (**28**) was prepared from commercially available phytosphingosine by following a reported method.⁵² Finally, the α -GalCer probes (**1–5**) were obtained by hydrogenation of compound **29**, followed by amide coupling with suitable carboxylic acids (**17**, **18**, **19**, **24**, and **25**) in the presence of HBTU and base in moderate yields.

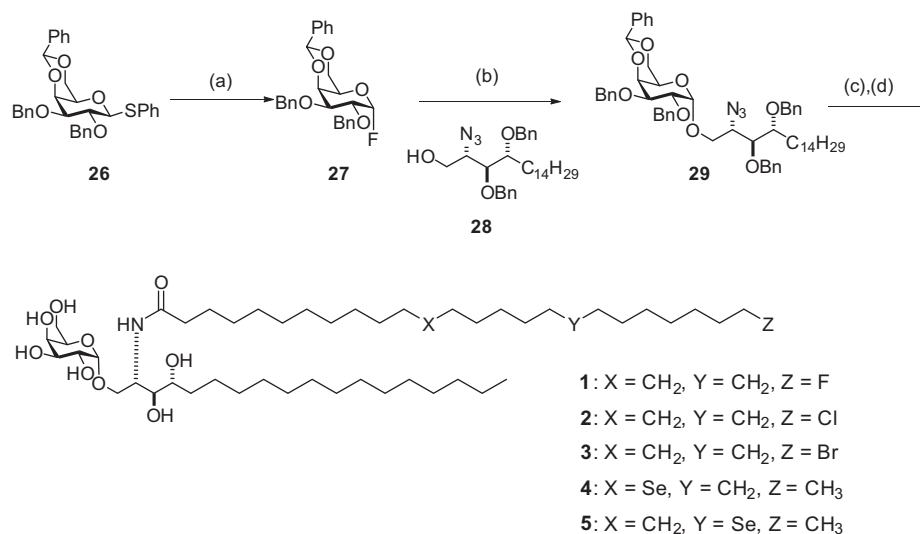
2.2. Cytokine production assay

To examine the immunostimulatory activity and Th1/Th2 selectivity of the synthetic α -GalCer analogues, cytokine productions were evaluated by using the primary culture of murine spleen cells with KRN7000 as a positive control (Fig. 3).⁵³ Five concentrations (10–1000 nM) of analogues **1–5** were incubated with freshly prepared mouse splenocytes and the amounts of cytokines produced after incubation for 48 hours were determined by ELISA kits. All of the compounds induced production of IFN- γ at a significant level (Fig. 3A). Fig. 3B shows the amounts of IL-4 produced in the presence of analogues **1–5**. Although they stimulated IL-4 production, their potency was grossly lower than KRN7000 in the concentrations tested. When the stimulation of the produced cytokines are compared at 100 nM with that of KRN7000 (Fig. 3C), all of the analogues showed higher selectivity toward IFN- γ production (IFN- γ /IL-4 = 2.9–5.0); in particular, analogue **1** showed the highest selectivity for IFN- γ production (IFN- γ /IL-4 = 5.0). This potency is comparable to the best IFN- γ selective ligand (IFN- γ /IL-4 = 5.80) reported so far.⁵⁴

3. Discussion

Our objective is to improve the accuracy of the 3D structure of the α -GalCer chain bound to the A' pocket of CD1d (Fig. 2). Toward this goal, we introduced a heavy atom into the acyl moiety of KRN7000 for enhancing the electron diffraction in X-ray crystallography. The high resolution crystal structure of the lipid binding pocket would disclose the atomistic mechanism of lipid-protein interactions and facilitate precise molecular designs for developing a more specific CD1d ligand.

In the cytokine production assays, the overall IFN- γ secretions induced by the synthetic analogues **1–5** showed a roughly similar rate to the standard KRN7000 (Fig. 3A). The result clearly indicates that all of our synthetic analogues form the bioactive ternary



Scheme 3. Reagents and conditions: (a) DAST, NBS, CH₂Cl₂, 40% (yield of α -anomer); (b) AgOTf, SnCl₂, MS 4Å, Et₂O/THF = 5, 0 °C, 73%; (c) 20% Pd(OH)₂-C, H₂, MeOH/CH₂Cl₂; (d) **17**, **18**, **19**, **24**, or **25**, HBTU, *N*-methylmorpholine, Et₃N, (40–60%).

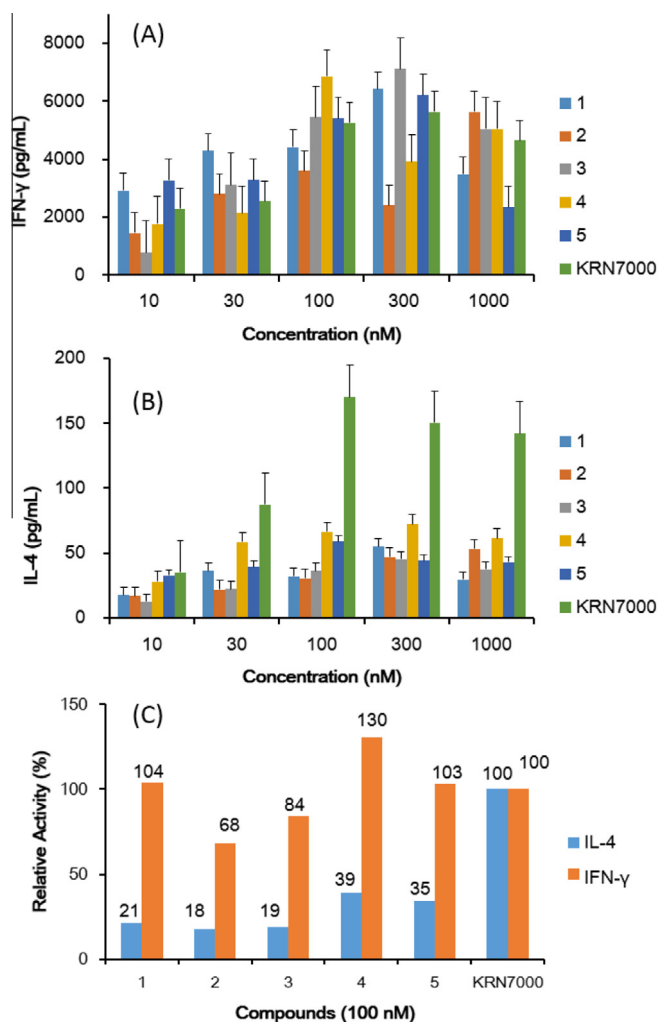


Figure 3. Cytokines produced due to the designed and synthesized α -GalCer analogues **1–5** by murine splenocytes. The amount of cytokine production, (pg/mL) of IFN- γ (A) and IL-4 (B) are summarized. (C) The relative rate of cytokine production of α -GalCers analogues against KRN7000, at 100 nM concentrations are summarized. IFN- γ /IL-4; **1**; 5.0, **2**; 3.8, **3**; 4.4, **4**; 3.3, **5**; 2.9.

complex with CD1d and TCR on NKT cells, and induce signaling cascades for cytokine production. The perturbation induced by a halogen atom at the C26' position or by a Se atom at C12' or C18' position is rather limited except for the reduced production of IL-4 at higher doses (Fig. 3B), where the cytokine level in the presence of the synthesized ligands was significantly lower than that of KRN7000. The Th1/Th2 selectivity is often discussed with the strength of the binding affinity of α -GalCer to CD1d, and of the CD1d/ α -GalCer complex to TCR.^{24,32,36} Liang et al. reported that the affinity between α -GalCer and CD1d correlates well with IFN- γ production by NKT cells, but less with IL-4 secretion.⁵⁵ Thus, similar IFN- γ production rates of the synthesized ligands (**1–5**) and KRN7000 imply their similar binding affinities to CD1d. According to the previous X-ray structure of the CD1d and KRN7000 complex, Koch et al. indicated that the binding of KRN7000 induces a slight closure of the ligand binding groove that consists of two α -helices.⁵ On the other hand, in the following complexation with TCR, the KRN7000/CD1d structure is unaltered—a lock and key type of interaction.^{6,32} Our synthetic analogues have all functional groups required for the interaction between KRN7000/CD1d and TCR, including 3-OH of sphingosine and 2''-OH, 3''-OH, and 4''-OH of galactose.³⁶ Therefore, our synthetic analogues in complex with CD1d would have similar conformation to that of KRN7000 in the bound form. These results imply that small changes in the bond lengths (C–X or C–Se vs C–C) or bond angle (C–Se–C vs C–C–C) in the modified sites of KRN7000 do not significantly affect their interaction mode. Thus, the X-ray co-crystallography of the synthetic analogues (**3**, **4**, and **5**) in complex with CD1d is most likely to mimic the ligand-binding mode of KRN7000 at the atomistic level, and the electron-poor acyl chain atom is expected to be clearly visualized by the electron-rich Br and Se atoms.

In contrast to the IFN- γ production, all of the analogues induced IL-4 secretion in smaller amounts as compared with KRN7000 under the middle and higher ligand concentrations (Fig. 3B). In other words, the significant suppression of the Th2 cytokine secretion makes the synthetic ligands biased toward IFN- γ production (Fig. 3C). The structural basis of the selectivity in the cytokine production has been speculated so far. As shown in Fig. 4, structural superposition of the Th1-selective ligand C8PhF⁵⁵ (PDB code: 3GMO)⁵⁶ and non-selective KRN7000 (PDB code: 3HE6)⁷ bound in a murine CD1d showed a slight difference. It is believed that the position of the sugar moiety, as the main recognition site by

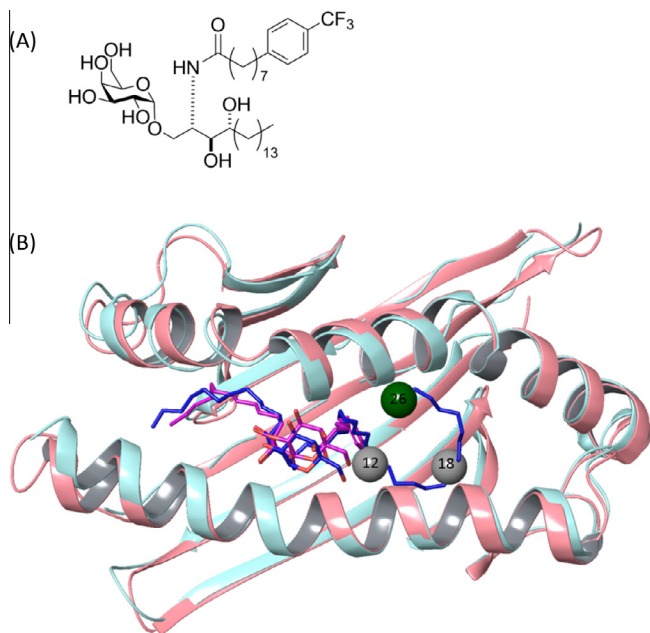


Figure 4. (A) Chemical structure of C8PhF, a Th1-selective ligand. (B) Superposed structures of murine CD1d complexed with Th1-selective ligand C8PhF (pink ribbon and magenta wire) and that with KRN7000 (sky-blue ribbon and blue wire); PDB codes are 3GMO and 3HE6. C26' of KRN7000 is shown with a dark green ball and C12'/C18' are shown with gray balls, which corresponded to halogen and selenium positions of the synthetic analogues, respectively.

TCR, influences the CD1d–TCR interaction, and consequently modulates the stability of the CD1d/ α -GalCer/TCR complex.^{6,32} In the CD1d–C8PhF complex, the modified acyl chain induces a small, but significant shift of the sugar moiety from the position found with KRN7000 (Fig. 4B). The cytokine assay results of a series of C8PhF-related compounds uniformly showed a reduction of IL-4 secretion, but a diverse response of IFN- γ secretion.⁵⁵ For analogues 1–5 that showed similar cytokine production profiles to that of C8PhF, interaction of the acyl chain with the A' pocket might be slightly weakened by the halogen or Se atom, and the resultant structural change could induce a slight shift in the position of the sugar head group upon the CD1d/ligand/TCR complexation, which possibly led to attenuation of the Th2 pathway. It is worth noting that a simple heavy atom substitution in the acyl chain of α -GalCers significantly influences the Th1/Th2 selectivity. Knowledge on structural basis in selective activation of iNKT cells potentially help develop drugs that modulate immune pathways including those necessary for cancer^{18,25} and malaria²⁹ treatments.

4. Conclusion

We established the synthesis of a novel class of α -GalCer probes bearing halogen-containing and selenium-containing fatty acid derivatives. The analogues showed efficient stimulation for IFN- γ secretion from murine spleen cells, which was comparable to KRN7000. The data suggests that synthetic analogues could be utilized to examine the atomistic interactions between KRN7000 and CD1d. The heavy atoms will help analyze the lipid–protein interactions by enhancing the poor electron density of the lipid tail. They will also be a good reporter in determining atomic positions precisely. Further study on X-ray crystallography is currently underway to elucidate the mechanism of atomistic interactions and the conformations of the α -GalCer ligands in the CD1d complex form.

5. Experimental

5.1. General

The commercially available reagents were used without further purification. The ¹H and ¹³C NMR spectra were measured on the ECA-500 and ECS-400 spectrometer (JEOL, Tokyo) with CDCl₃ as a solvent unless otherwise indicated. Chemical shifts are given in ppm (δ) and coupling constants (J) are in Hz. The following abbreviations were used to designate the multiplicities: s = singlet, d = doublet, t = triplet, q = quartet, quint = quintuplet, m = multiplet, br = broad. High resolution mass spectra were obtained on LTQ-Orbitrap XL mass spectrometer (Thermo Scientific, CA).

5.2. Synthetic procedures

5.2.1. 5-(12-*tert*-Butyldimethylsilyloxydodecylthio)-1-phenyl-1H-tetrazole (7)

To a solution of **6** (2.04 g, 6.45 mmol) in THF (30 mL) added PPh₃ (2.03 g, 7.74 mmol), diethyl azodicarboxylate (1.35 mL; 2.2 M solution in toluene, 7.74 mmol), and 1-phenyl-1H-tetrazole-5-thiol (1.38 g, 7.74 mmol) at 0 °C was stirred for 2 h at room temperature under argon atmosphere. Then, the mixture was diluted with Et₂O and the organic phase was washed with water and brine, dried over MgSO₄, filtered and concentrated. The crude residue was purified by silica gel column chromatography (4% EtOAc in hexane) to afford **7** (2.94 g, 6.19 mmol, 96%) as a sticky mass. ¹H NMR (500 MHz, CDCl₃) δ 7.62–7.48 (m, 5H), 3.58 (t, *J* = 6.6 Hz, 2H), 3.42–3.34 (m, 2H), 1.80 (dt, *J* = 15.0, 7.5 Hz, 2H), 1.54–1.46 (m, 2H), 1.46–1.37 (m, 2H), 1.35–1.19 (m, 14H), 0.88 (s, 9H), 0.03 (s, 6H); ¹³C NMR (126 MHz, CDCl₃) δ 154.55, 133.8, 130.1, 129.8, 123.9, 63.4, 33.5, 32.9, 29.7, 29.6, 29.5, 29.2, 29.1, 28.7, 26.1, 25.9, 18.4, –5.1; HRMS calculated for C₂₅H₄₄N₄OSSiNa: 499.3005, found 499.3002 [M+Na]⁺.

5.2.2. 5-(12-*tert*-Butyldimethylsilyloxydodecylsulfonyl)-1-phenyl-1H-tetrazole (8)

m-Chloroperoxybenzoic acid (75%, 7.15 g, 31.05 mmol) was added to the solution of **7** (2.59 g, 6.21 mmol) in CH₂Cl₂ (70 mL) at 0 °C under argon atmosphere. After the reaction mixture was stirred overnight at room temperature, 10% aq Na₂S₂O₃ (15 mL) was added and stirred for additional 30 min. Sat. NaHCO₃ (20 mL) was added before extraction with CH₂Cl₂. The organic phase was washed sequentially with 10% aq Na₂S₂O₃, sat NaHCO₃, and brine. The organic phase was dried over Na₂SO₄, filtered, and filtrate was evaporated and the residue was purified by silica gel column chromatography (3% EtOAc in hexane) to afford **8** (2.66 g, 5.24 mmol, 84%) as a white solid. ¹H NMR (500 MHz, CDCl₃) δ 7.72–7.66 (m, 2H), 7.66–7.55 (m, 3H), 3.75–3.68 (m, 2H), 3.59 (t, *J* = 6.6 Hz, 2H), 1.99–1.90 (m, 2H), 1.49 (s, 4H), 1.38–1.21 (m, 14H), 0.89 (s, 9H), 0.04 (s, 6H); ¹³C NMR (126 MHz, CDCl₃) δ 153.6, 133.1, 131.5, 129.8, 125.1, 63.4, 56.1, 32.1, 29.7, 29.6, 29.5, 29.3, 29.0, 28.3, 26.1, 25.9, 22.1, 18.5, –5.1; HRMS calculated for C₂₅H₄₄N₄O₃SSiNa: 531.2903, found 531.2903 [M+Na]⁺.

5.2.3. 13-Benzyloxy-13-oxotridecanoic acid (9)

To a solution of tridecanedioic acid (5.0 g, 20.5 mmol) in THF (30 mL) at 0 °C added benzylbromide (2.44 mL, 20.5 mmol) and diazabicyclo[5.4.0]undec-7-ene (3.05 mL, 20.5 mmol) was stirred at room temperature for overnight. Then, water was added, and the reaction mixture was extracted with EtOAc, dried over MgSO₄, filtered, and concentrated. The crude residue was purified by silica gel column chromatography (16% EtOAc in hexane) to afford **9** (3.10 g, 9.42 mmol, 46%) as a white solid. ¹H NMR (400 MHz, CDCl₃) δ 7.41–7.28 (m, 5H), 5.11 (s, 2H), 2.34 (td, *J* = 7.5, 2.9 Hz,

4H), 1.62 (dt, $J = 15.0, 7.3$ Hz, 4H), 1.39–1.19 (m, 14H); ^{13}C NMR (101 MHz, CDCl_3) δ 179.8, 173.8, 136.2, 128.6, 128.2, 66.2, 34.5, 34.1, 29.39, 25.1, 24.7; HRMS calculated for $\text{C}_{20}\text{H}_{30}\text{O}_4\text{Na}$: 357.2144, found 357.2141 $[\text{M}+\text{Na}]^+$.

5.2.4. Benzyl 13-hydroxytridecanoate (10)

A solution of **9** (2.69 g, 8.05 mmol) in THF (20 mL) was cooled at 0 °C and borane-tetrahydrofuran complex (1 M solution in THF, 16 mL) was added over 20 min with maintaining the cooling temperature. After stirring at room temperature for 2 h, the reaction mixture was quenched with water, extracted with EtOAc, dried over MgSO_4 , filtered, and concentrated. The crude residue was purified by silica gel column chromatography (16% EtOAc in hexane) to afford **10** (2.12 g, 6.61 mmol, 82%) as a white solid. ^1H NMR (500 MHz, CDCl_3) δ 7.40–7.28 (m, 5H), 5.11 (s, 2H), 3.63 (t, $J = 6.6$ Hz, 2H), 2.34 (t, $J = 7.5$ Hz, 2H), 1.69–1.59 (m, 2H), 1.59–1.51 (m, 2H), 1.39–1.20 (m, 16H); ^{13}C NMR (126 MHz, CDCl_3) δ 173.8, 136.2, 66.2, 63.2, 34.5, 34.5, 32.9, 32.9, 29.6, 29.5, 29.3, 29.2; 25.8, 25.0 HRMS calculated for $\text{C}_{20}\text{H}_{32}\text{O}_3\text{Na}$: 343.2351, found 343.2345 $[\text{M}+\text{Na}]^+$.

5.2.5. Benzyl 13-oxotridecanoate (11)

To a solution of **10** (2.65 g, 8.28 mmol) in dichloromethane (50 mL) at 0 °C added pyridinium chlorochromate (3.41 g, 15.81 mmol), and sodium acetate (339 mg, 4.14 mmol) was stirred overnight at room temperature. Then, the precipitate was separated by filtration and washed with EtOAc. The filtrate was concentrated and purified by silica gel column chromatography (8% EtOAc in hexane) to afford **11** (2.12 g, 6.67 mmol, 80%) as an oil. ^1H NMR (500 MHz, CDCl_3) δ 9.75 (s, 1H), 7.42–7.28 (m, 5H), 5.11 (s, 2H), 2.41 (t, $J = 7.4$ Hz, 2H), 2.34 (t, $J = 7.5$ Hz, 2H), 1.62 (dd, $J = 14.6, 7.3$ Hz, 4H), 1.36–1.19 (m, 14H); ^{13}C NMR (126 MHz, CDCl_3) δ 202.8, 173.6, 136.0, 128.4, 128.1, 66.0, 43.8, 34.3, 29.4, 29.3, 29.3, 29.1, 29.1, 29.0, 24.9, 22.0; HRMS calculated for $\text{C}_{20}\text{H}_{30}\text{O}_3\text{Na}$: 341.2195, found 341.2185 $[\text{M}+\text{Na}]^+$.

5.2.6. Benzyl 25-(tert-butyl dimethylsilyloxy)pentacos-13-enoate (12)

A solution of **8** (1.79 g, 3.53 mmol) and **11** (1.36 g 4.27 mmol) in THF was cooled at –78 °C and LiHMDS (1 M in THF, 3.53 mL) was added over 15 min under argon atmosphere. After stirring for 3 h, the reaction mixture was warmed up and stirred overnight at room temperature. The reaction mixture was quenched with NH_4Cl solution and extracted with Et_2O . After removal of the solvent, the residue was purified by silica gel column chromatography (2% EtOAc in hexane) to afford **12** (1.7 g, 2.83 mmol, 80%) as an oil. ^1H NMR (500 MHz, CDCl_3) δ 7.40–7.27 (m, 5H), 5.38 (t, $J = 3.7$ Hz, trace), 5.35 (t, $J = 5$ Hz, trace), 5.11 (s, 2H), 3.60 (t, $J = 6.7$ Hz, 2H), 2.35 (t, $J = 7.5$ Hz, 2H), 1.96 (dt, $J = 7.3, 3.6$ Hz, 4H), 1.70–1.59 (m, 2H), 1.55–1.47 (m, 2H), 1.37–1.20 (m, 32H), 0.92–0.87 (m, 9H), 0.06–0.03 (m, 6H); ^{13}C NMR (126 MHz, CDCl_3) δ 173.7, 136.2, 130.4, 129.9, 128.6, 128.2, 66.1, 63.4, 34.4, 33.0, 32.7, 29.9, 29.7, 29.7, 29.6, 29.5, 29.4, 29.3, 29.3, 29.2, 27.3, 26.1, 25.9, 25.0, 18.5, –5.1; HRMS calculated for $\text{C}_{38}\text{H}_{68}\text{O}_5\text{SiNa}$: 623.4938, found 623.4939 $[\text{M}+\text{Na}]^+$.

5.2.7. Benzyl 25-hydroxypentacos-13-enoate (13)

To a solution of **12** (358 mg, 0.596 mmol) in THF added TBAF (1 M in THF, 894 μL) at 0 °C was stirred overnight at room temperature. Then, solvent was evaporated and the residue was purified by silica gel column chromatography (16% EtOAc in hexane) to afford **13** (231 mg, 0.48 mmol, 80%) as a sticky mass. ^1H NMR (500 MHz, CDCl_3) δ 7.39–7.29 (m, 5H), 5.38 (t, $J = 3.7$ Hz, trace), 5.34 (t, $J = 4.5$ Hz, trace), 5.11 (s, 2H), 3.63 (t, $J = 6.6$ Hz, 2H), 2.35 (t, $J = 7.5$ Hz, 2H), 1.97 (ddd, $J = 12.4, 10.0, 3.4$ Hz, 4H), 1.62 (dd,

$J = 14.7, 7.3$ Hz, 2H), 1.55 (dt, $J = 13.3, 6.7$ Hz, 2H), 1.43–1.20 (m, 32H); ^{13}C NMR (126 MHz, CDCl_3) δ 173.7, 136.2, 130.4, 129.9, 128.6, 128.2, 66.1, 63.2, 34.5, 29.9, 29.8, 29.7, 29.6, 29.6, 29.4, 29.6, 29.26 (d), 27.3, 25.9, 25.1; HRMS calculated for $\text{C}_{32}\text{H}_{54}\text{O}_3\text{Na}$: 509.4073, found 509.4071 $[\text{M}+\text{Na}]^+$.

5.2.8. Benzyl 25-(methylsulfonyloxy)pentacos-13-enoate (14)

To a solution of **13** (510 mg, 1.1 mmol) in pyridine (6.5 mL) and THF (10 mL) added methanesulfonyl chloride (297 μL , 3.83 mmol) at 0 °C was stirred overnight at room temperature. Then, solvent was evaporated and the residue was purified by silica gel column chromatography (10% EtOAc in hexane and 50% EtOAc in hexane) to afford **14** (588 mg, 1.04 mmol, 94%) as a sticky mass. ^1H NMR (500 MHz, CDCl_3) δ 7.40–7.28 (m, 5H), 5.41–5.32 (m, 2H), 5.11 (s, 2H), 4.21 (t, $J = 6.6$ Hz, 2H), 2.99 (s, 3H), 2.34 (t, $J = 7.6$ Hz, 2H), 2.03–1.92 (m, 4H), 1.79–1.69 (m, 2H), 1.68–1.57 (m, 2H), 1.43–1.14 (m, 32H); ^{13}C NMR (126 MHz, CDCl_3) δ 173.5, 140.5, 130.3, 128.5, 128.1, 70.1, 66.0, 37.3, 34.3, 32.6, 29.7, 29.6, 29.6, 29.5, 29.5, 29.4, 29.4, 29.3, 29.2, 29.1, 29.1, 29.0, 25.4, 24.9; HRMS calculated for $\text{C}_{33}\text{H}_{56}\text{O}_5\text{SNa}$: 587.3848, found 587.3743 $[\text{M}+\text{Na}]^+$.

5.2.9. Benzyl 25-fluoropentacos-13-enoate (15)

To a solution of **13** (100 mg, 0.22 mmol) in CH_2Cl_2 (10 mL) added diethylaminosulfur trifluoride (DAST; 48 μL , 0.39 mmol) at 0 °C was stirred for 5 h at room temperature. Then, solvent was evaporated and the residue was purified by silica gel column chromatography (4% EtOAc in hexane) to afford **15** (76 mg, 0.16 mmol, 71%) as a white solid. ^1H NMR (500 MHz, CDCl_3) δ 7.40–7.28 (m, 5H), 5.38 (t, $J = 3.7$ Hz, trace), 5.34 (t, $J = 4.5$ Hz, trace), 5.11 (s, 2H), 4.43 (dt, $J = 47.4, 6.2$ Hz, 2H), 2.34 (t, $J = 7.5$ Hz, 2H), 2.04–1.92 (m, 4H), 1.74–1.59 (m, 4H), 1.45–1.20 (m, 32H); ^{13}C NMR (126 MHz, CDCl_3) δ 173.7, 136.2, 130.4, 129.96, 128.6, 128.2, 84.3 ($J_{\text{C-F}} = 164.1$ Hz), 66.1, 34.5, 32.7, 30.6, 30.5, 29.9, 29.8, 29.7, 29.6, 29.6, 29.4, 29.3, 27.3, 25.3, 25.2, 25.1; HRMS calculated for $\text{C}_{32}\text{H}_{53}\text{FO}_2\text{Na}$: 511.4030, found 511.4026 $[\text{M}+\text{Na}]^+$.

5.2.10. 25-((Methylsulfonyl)oxy)pentacosanoic acid (16)

To a solution of **14** (240 mg, 0.53 mmol) in $\text{CH}_2\text{Cl}_2/\text{MeOH}$ (5:3 v/v, 10 mL) added $\text{Pd}(\text{OH})_2$ (20 wt%, 240 mg) and triethylsilane (0.84 mL, 5.3 mmol) was stirred at room temperature for 30 min. Then, the catalyst was removed by filtration through Celite pad, and filtrate was evaporated and the residue was purified by silica gel column chromatography (10% MeOH in CH_2Cl_2) to afford **16** (155 mg, 0.43 mmol, 80%) as a white solid. ^1H NMR (500 MHz, CDCl_3) δ 4.21 (t, $J = 6.6$ Hz, 2H), 2.98 (s, 3H), 2.34 (t, $J = 7.5$ Hz, 2H), 1.74 (dt, $J = 14.6, 6.7$ Hz, 2H), 1.62 (dd, $J = 14.9, 7.3$ Hz, 2H), 1.45–1.36 (m, 2H), 1.31 (d, $J = 54.7$ Hz, 40H); ^{13}C NMR (126 MHz, CDCl_3) δ 178.5, 70.1, 37.3, 33.8, 29.7, 29.5, 29.4, 29.3, 29.2, 29.1, 29.0, 25.4, 24.7; HRMS calculated for $\text{C}_{26}\text{H}_{52}\text{O}_5\text{SNa}$: 499.3535, found 499.3539 $[\text{M}+\text{Na}]^+$.

5.2.11. 25-Fluoropentacosanoic acid (17)

To a solution of **15** (76 mg, 0.16 mmol) in $\text{CH}_2\text{Cl}_2/\text{MeOH}$ (5:3 v/v; 5 mL) added $\text{Pd}(\text{OH})_2$ (20 wt%, 76 mg) and triethylsilane (299 μL , 1.6 mmol) was stirred for 30 min at room temperature. Then, the catalyst was removed by filtration through Celite pad, and filtrate was concentrated and the residue was purified by silica gel column chromatography (10% MeOH in CH_2Cl_2) to afford **17** (56 mg, 0.14 mmol, 85%) as a white solid. ^1H NMR (300 MHz, CDCl_3) δ 4.43 (dt, $J = 47.4, 6.2$ Hz, 2H), 2.34 (t, $J = 7.5$ Hz, 2H), 1.77–1.54 (m, 4H), 1.49–1.17 (m, 40H); ^{13}C NMR (126 MHz, CDCl_3) δ 175.3, 82.0 ($J_{\text{C-F}} = 163.8$ Hz) 34.2, 32.9, 29.6, 29.3, 29.2, 28.9, 28.3, 24.8; HRMS calculated for $\text{C}_{25}\text{H}_{49}\text{FO}_2\text{Na}$: 423.3717, found 423.3716 $[\text{M}+\text{Na}]^+$.

5.2.12. 25-Chloropentacosanoic acid (**18**)

To a solution of **17** (60 mg, 0.109 mmol) in toluene/H₂O = 2:3 (1.5 mL) added KCl (203.1 mg, 2.72 mmol) and tetrabutylammonium hydrogensulfate (12.95 mg, 0.038 mmol) was heated at 100 °C for 4 h. Then, the reaction mixture was cooled to room temperature, solvent was removed and the residue was purified by silica gel column chromatography (2% MeOH in CH₂Cl₂) to afford **18** (40 mg, 0.098 mmol, 90%) as a white solid. ¹H NMR (400 MHz, CDCl₃) δ 3.52 (t, *J* = 6.8 Hz, 2H), 2.34 (t, *J* = 7.5 Hz, 2H), 1.83–1.70 (m, 2H), 1.62 (dd, *J* = 14.8, 7.3 Hz, 2H), 1.41 (dd, *J* = 10.1, 5.1 Hz, 2H), 1.37–1.17 (m, 38H); ¹³C NMR (101 MHz, CDCl₃) δ 178.4, 45.2, 33.7, 32.6, 29.8, 29.7, 29.6, 29.5, 29.4, 29.2, 29.0, 28.9, 26.8, 24.6; HRMS calculated for C₂₅H₄₉ClO₂Na: 439.3421, found 439.3420 [M+Na]⁺.

5.2.13. 25-Bromopentacosanoic acid (**19**)

To a solution of **17** (50 mg, 0.105 mmol) in toluene/H₂O = 2:3 (1.5 mL) added KBr (119 mg, 2.62 mmol) and tetrabutylammonium hydrogensulfate (12.5 mg, 0.037 mmol) was heated at 100 °C for 4 h. Then, the mixture was cooled to room temperature, solvent was removed, and the residue was purified by silica gel column chromatography (2% MeOH in CH₂Cl₂) to afford **19** (45 mg, 0.098 mmol, 93%) as a white solid. ¹H NMR (500 MHz, CDCl₃) δ 3.40 (t, *J* = 6.9 Hz, 2H), 2.35 (t, *J* = 7.5 Hz, 2H), 1.85 (dt, *J* = 8.9, 6.9 Hz, 2H), 1.63 (dt, *J* = 15.0, 7.5 Hz, 2H), 1.41 (dd, *J* = 9.2, 4.3 Hz, 2H), 1.35–1.21 (m, 38H); ¹³C NMR (126 MHz, CDCl₃) δ 180.5, 34.0, 33.7, 32.8, 32.3, 31.5, 29.7, 29.6, 29.5, 29.2, 29.0, 28.7, 24.7; HRMS calculated for C₂₅H₄₉BrO₂Na: 483.2916, found 483.2914 [M+Na]⁺.

5.2.14. Dioctyldiselenide (**20**)

Elemental selenium (147.5 mg, 1.87 mmol) was suspended in ethanol (6 mL) and NaBH₄ was slowly added (297.4 mg, 7.86 mmol) under argon atmosphere while H₂ gas was evolved vigorously. The mixture was stirred until complete dissolution of selenium. Second portion of the elemental selenium (147.5 mg, 1.87 mmol) was then added and the mixture was stirred for 20 min at room temperature, and followed by heating at 65 °C for 5 min with continuous argon bubbling. 1-Bromooctane (719 mg, 3.74 mmol) was then slowly added under vigorous stirring and the mixture was stirred for 1 h at 65 °C. Then, the reaction mixture was filtered and the residue was washed with hexane. The filtrate was concentrated and the crude residue was purified by chromatography on silica gel (hexane) to afford **20** (450 mg, 1.17 mmol, 62%) as a sticky mass. ¹H NMR (400 MHz, CDCl₃) δ 3.13–3.04 (m, 1H), 2.95–2.85 (m, 3H), 1.80 (dt, *J* = 14.9, 7.3 Hz, 1H), 1.77–1.67 (m, 3H), 1.32 (m, 20H), 0.88 (t, *J* = 6.9 Hz, 6H); ¹³C NMR (101 MHz, CDCl₃) δ 31.8, 31.0, 30.5, 30.3, 29.5, 29.2, 29.1, 22.6, 14.1; HRMS calculated for C₁₆H₃₄Se₂Na: 509.0991, found 509.0990 [M+Na]⁺.

5.2.15. 11-(Tetradecylselenyl)undecanoic acid (**24**)

To synthesize compound **24**, 1-bromotetradecane was transformed into diselenide **21** by following the procedure as of compound **20**. Without further purification, the ditetradecyldiselenide **21** was used for the reaction with carboxylic acid **22** in a manner similar to that described for compound **25** to give **24** (42%, white solid). ¹H NMR (400 MHz, CDCl₃) δ 2.54 (t, *J* = 7.5 Hz, 4H), 2.34 (t, *J* = 7.5 Hz, 2H), 1.63 (m, 7.3 Hz, 6H), 1.45–1.18 (m, 34H), 0.87 (t, *J* = 6.8 Hz, 3H); ¹³C NMR (101 MHz, CDCl₃) δ 178.9, 33.8, 31.8, 30.7, 30.0, 29.6, 29.5, 29.4, 29.2, 29.1, 29.0, 24.7, 24.0, 22.6, 14.1.

5.2.16. 17-(Octylselenyl)heptadecanoic acid (**25**)

A solution of NaBH₄ (22.7 mg, 0.6 mmol) in THF/water 1:1 (0.072 mL) was added to a solution of **20** (45 mg, 0.12 mmol) in THF (0.5 mL), and the mixture was stirred until the solution

became colorless. A solution of 17-bromoheptadecanoic acid (**23**) (150 mg, 0.42 mmol) and triethylamine (0.069 mL, 0.48 mmol) in water (0.5 mL) was added dropwise and the mixture was stirred overnight. The mixture was then quenched with 4 M HCl and extracted with Et₂O (×3). Combined organic layers were washed with brine, dried over MgSO₄, filtered, and concentrated. The crude residue was purified by chromatography on silica gel (gradient hexane/EtOAc 10:0 to 5:5) to afford 17-(octylselenyl)heptadecanoic acid **25** (80 mg, 0.173 mmol, 42%) as a white solid. ¹H NMR (400 MHz, CDCl₃) δ 2.54 (t, *J* = 7.5 Hz, 4H), 2.34 (t, *J* = 7.5 Hz, 2H), 1.63 (m, 7.3 Hz, 6H), 1.45–1.18 (m, 34H), 0.87 (t, *J* = 6.8 Hz, 3H); ¹³C NMR (101 MHz, CDCl₃) δ 179.0, 33.9, 31.9, 30.8, 30.1, 29.7, 29.3, 24.8, 24.1, 22.7, 14.2; HRMS calculated for C₂₅H₅₀O₂SeNa: 485.2976, found [M+Na] 485.2975.

5.2.17. (2-Azido-3,4-di-*O*-benzyl-1-*O*-(2,3-di-*O*-benzyl-4,6-*O*-benzylidene- α -*D*-galactopyranosyl)-*D*-ribo-octadecane-1,3,4-triol (**29**)

A mixture of **28** (1.74 g, 3.32 mmol) and **27** (1.63 g, 3.62 mmol) was co-evaporated with toluene and dissolved in Et₂O/THF = 5:1 (72 mL) dried with MS 4Å under argon atmosphere. AgOTf (2.58 g, 10.05 mmol) and SnCl₂ (1.2 g, 6.36 mmol) were added to the reaction mixture at 0 °C. After stirring for 2 h at 0 °C, the TLC analysis (6% hexane in EtOAc) of the reaction mixture shows full consumption of compound **27**. The reaction was quenched with sat. NaHCO₃ and extracted with EtOAc, and the organic phase was washed with brine, dried over MgSO₄, filtered, and concentrated under reduced pressure. The crude residue was purified by silica gel column chromatography (7% EtOAc in hexane) to afford **29** (1.53 g, 1.72 mmol, 73%) as a white solid. ¹H NMR (500 MHz, CDCl₃) δ 7.51 (dd, *J* = 7.7, 1.8 Hz, 2H), 7.42–7.19 (m, 23H), 5.45 (s, 1H), 4.96 (d, *J* = 3.4 Hz, 1H), 4.83 (m, 2H), 4.73 (d, *J* = 12.3 Hz, 1H), 4.70–4.62 (m, 2H), 4.58 (dd, *J* = 13.7, 9.6 Hz, 2H), 4.49 (d, *J* = 11.5 Hz, 1H), 4.17–4.14 (m, 1H), 4.11–3.97 (m, 3H), 3.92–3.85 (m, 1H), 3.80 (s, 1H), 3.66 (m, 5H), 1.75–1.60 (m, 1H), 1.54 (s, 2H), 1.48–1.35 (m, 1H), 1.35–1.08 (m, 23H), 0.88 (t, *J* = 6.9 Hz, 3H).

5.2.18. General procedure for amide coupling reaction

2 equiv of HBTU, Et₃N, and *N*-methylmorpholine were added to the solution of deprotected galactosyl sphingosine **29** and one of the long chain fatty acid (**17**, **18**, **19**, **24** and **25**) in THF. The reaction mixture was stirred overnight at room temperature. Upon full consumption of starting materials confirmed by TLC analysis, the crude residue was concentrated and purified by chromatography on silica gel (MeOH/CH₂Cl₂ = 10:1) to afford the corresponding amides.

5.2.19. 1-*O*- α -*D*-Galactopyranosyl-2-*N*-(25-fluoropentacosanoyl)-2S,3S,4R-phytosphingosine (**1**)

(15 mg, 17.42 μ mol 53%), white solid; ¹H NMR (500 MHz, CDCl₃, CD₃OD) δ 4.88 (d, *J* = 3.8 Hz, 1H), 4.45 (t, *J* = 6.2 Hz, 1H), 4.35 (t, *J* = 6.2 Hz, 1H), 4.23–4.14 (m, 1H), 3.88 (ddd, *J* = 15.2, 6.9, 2.7 Hz, 2H), 3.84–3.77 (m, 2H), 3.77–3.65 (m, 4H), 3.62–3.50 (m, 2H), 2.21 (t, *J* = 7.6 Hz, 2H), 1.79–1.53 (m, 6H), 1.48–1.18 (m, 67H), 0.88 (t, *J* = 7.0 Hz, 3H); ¹³C NMR (126 MHz, CDCl₃, CD₃OD) δ 180.6, 99.8, 83.4 (*J*_{C-F} = 163.5 Hz) 75.1, 74.2, 73.8, 71.2, 70.2, 69.7, 68.9, 67.1, 61.5, 37.7, 36.0, 31.7, 30.3, 30.2, 29.6, 29.5, 29.4, 29.3, 29.2, 29.1, 29.0, 25.7, 22.4, 13.2, 8.0; HRMS calculated for C₄₉H₉₆FNO₉Na: 884.7069, found 884.7065 [M+Na]⁺.

5.2.20. 1-*O*- α -*D*-Galactopyranosyl-2-*N*-(25-chloropentacosanoyl)-2S,3S,4R-phytosphingosine (**2**)

(15 mg, 17.09 μ mol, 53%), white solid; ¹H NMR (400 MHz, CDCl₃) δ 4.85 (d, *J* = 3.8 Hz, 1H), 4.21–4.12 (m, 1H), 3.90–3.64 (m, 2H), 3.63–3.57, 3.52 (t, *J* = 4.0 Hz, 2H), 2.20 (t, *J* = 7.7 Hz, 2H), 1.78–1.68 (m, 2H), 1.68–1.52 (m, 4H), 1.47–1.37 (m, 3H),

1.37–1.05 (m, 54H), 0.88 (t, $J = 6.9$ Hz, 3H); ^{13}C NMR (101 MHz, CDCl_3) δ 162.8, 56.2, 47.0, 46.2, 43.8, 43.7, 43.6, 43.4, 43.3, 43.1, 41.5, 39.8, 31.3, 20.58, 17.87, 8.80; HRMS calculated for $\text{C}_{49}\text{H}_{96}\text{ClNO}_9\text{Na}$: 900.6774, found 900.6771 $[\text{M}+\text{Na}]^+$.

5.2.21. 1-*O*- α -D-Galactopyranosyl-2-*N*-(25-bromopentacosanoyl)-2*S*,3*S*,4*R*-phytosphingosine (3)

(15 mg, 16.24 μmol , 43%), white solid; ^1H NMR (400 MHz, CDCl_3 , CD_3OD) δ 4.91 (d, $J = 3.8$ Hz, 1H), 4.20 (d, $J = 4.6$ Hz, 1H), 4.03–3.86 (m, 2H), 3.84–3.71 (m, 6H), 3.55 (d, $J = 4.0$ Hz, 2H), 3.50–3.37 (m, 2H), 3.39–3.27 (m, 2H), 2.21 (t, $J = 7.7$ Hz, 2H), 1.99–1.76 (m, 2H), 1.73–1.50 (m, 4H), 1.43 (d, $J = 7.5$ Hz, 3H), 1.28 (d, $J = 11.3$ Hz, 59H), 0.89 (t, $J = 6.9$ Hz, 3H); ^{13}C NMR (101 MHz, CDCl_3 , CD_3OD) δ 174.1, 99.4, 74.4, 71.6, 70.4, 69.9, 69.4, 68.6, 67.0, 61.5, 50.1, 36.1, 33.5, 32.5, 32.2, 31.5, 29.3, 29.1, 29.0, 28.9, 28.3, 27.7, 25.4, 22.2, 13.5; HRMS calculated for $\text{C}_{49}\text{H}_{96}\text{BrNO}_9\text{Na}$: 946.2090, found 946.2099 $[\text{M}+\text{Na}]^+$.

5.2.22. 1-*O*- α -D-Galactopyranosyl-2-*N*-(11-tetradecylselenoundecanoyl)-2*S*,3*S*,4*R*-phytosphingosine (4)

(13 mg, 14.07 μmol , 45%) white solid; ^1H NMR (500 MHz, CD_3OD) δ 4.85 (d, $J = 3.7$ Hz, 1H), 4.17 (dt, $J = 6.3$, 4.5 Hz, 1H), 3.89–3.83 (m, 2H), 3.81 (t, $J = 6.0$ Hz, 1H), 3.79–3.49 (m, 7H), 2.52 (t, $J = 7.4$ Hz, 4H), 2.20 (t, $J = 7.5$ Hz, 2H), 1.67–1.45 (m, 9H), 1.45–1.06 (m, 68H), 0.88 (t, $J = 6.9$ Hz, 6H); ^{13}C NMR (126 MHz, CD_3OD) δ 174.4, 99.8, 74.0, 71.6, 71.2, 70.2, 69.7, 68.9, 67.0, 61.4, 50.6, 35.9, 31.7, 31.5, 30.4, 30.4, 29.6, 29.5, 29.4, 29.3, 29.3, 29.2, 29.1, 28.9, 28.8, 25.7, 23.1, 22.4, 13.1; HRMS calculated for $\text{C}_{49}\text{H}_{97}\text{NO}_9\text{SeNa}$: 946.6329, found 946.6331 $[\text{M}+\text{Na}]^+$.

5.2.23. 1-*O*- α -D-Galactopyranosyl-2-*N*-(17-octylselenoheptadecanoyl)-2*S*,3*S*,4*R*-phytosphingosine (5)

(12 mg, 12.99 μmol , 40%) white solid; ^1H NMR (500 MHz, CD_3OD) δ 4.88 (d, $J = 3.8$ Hz, 1H), 4.19 (d, $J = 5.3$ Hz, 1H), 3.94–3.83 (m, 2H), 3.83–3.75 (m, 2H), 3.75–3.64 (m, 4H), 3.62–3.51 (m, 2H), 2.54 (t, $J = 7.4$ Hz, 4H), 1.64 (dd, $J = 14.9$, 7.5 Hz, 8H), 1.44–1.13 (m, 61H), 0.88 (t, $J = 6.7$ Hz, 6H); ^{13}C NMR (126 MHz, CD_3OD) δ 174.5, 99.1, 73.7, 71.1, 70.4, 69.6, 69.0, 68.3, 66.5, 61.0, 49.8, 35.6, 33.6, 31.2, 31.1, 29.9, 29.1, 29.0, 28.9, 28.9, 28.8, 28.7, 28.7, 28.6, 28.4, 26.2, 25.2, 25.0, 22.9, 21.9, 12.9. HRMS calculated for $\text{C}_{49}\text{H}_{97}\text{NO}_9\text{SeNa}$: 946.6329, found 946.6325 $[\text{M}+\text{Na}]^+$.

5.3. Cytokine production assay using murine spleen cell

Production of IFN- γ and IL-4 were examined using murine spleen cell.^{40,53} Murine spleen cell were collected from 6 female C57BL/6 mice. The mice were sacrificed and the spleens were immediately collected and passed through Cell strainer to give cell suspension in media. The cells were washed three times by centrifugation (1000 rpm, 10 $^\circ\text{C}$, 5 min) using media, and the resulting pellet was re-suspended, and cell number was counted using Türk's solution. Finally, the concentration of the cell were adjusted to 1.5×10^6 cells/mL and seeded into 96 well plate with 200 μL each (3×10^5 cells/well) in RPMI1640 medium (Sigma–Aldrich) including 10% FBS and 1% penicillin–streptomycin solution ($\times 100$ conc., Gibco). KRN7000 (Funakoshi Co. Ltd, Tokyo) and synthetic α -GalCer probes were diluted with pyridine (1 mg/mL) and further dilution using the media to be 0.1, 0.3, 1.0, 3.0, and 10 μM , respectively. The diluted sample solutions (20 μL) were added to the 96-well cell culture plate and the final concentration was fixed as 10, 30, 100, 300, and 1000 nM, respectively. The plates were incubated for 48 h at 37 $^\circ\text{C}$, and then centrifuged (3000 rpm, 4 $^\circ\text{C}$, 10 min). The supernatants were collected and the amounts of IFN- γ and IL-4 are measured by ELISA assay kits (Thermo Scientific, MA) according to the general procedures.

Acknowledgements

We thank Mr. Y. Shibata for his help in organic synthesis, Drs. Y. Todokoro, N. Inazumi, and A. Ito for maintenance and measurements for NMR and MS, and Mr. D. Takahashi and his colleague (KAC Inc., Kyoto, Japan) for bioassay. This work was supported in part by Japan Science and Technology Agency (JST) ERATO, Lipid Active Structure Project and by JSPS KAKENHI Grant Numbers 26560448, 25242073 and 15K01801.

Supplementary data

Supplementary data associated with this article can be found, in the online version, at <http://dx.doi.org/10.1016/j.bmc.2016.06.007>.

References and notes

- Natori, T.; Koezuka, Y.; Higa, T. *Tetrahedron Lett.* **1993**, *34*, 5591.
- Natori, T.; Morita, M.; Akimoto, K.; Koezuka, Y. *Tetrahedron* **1994**, *50*, 2771.
- Morita, M.; Motoki, K.; Akimoto, K.; Natori, T.; Sakai, T.; Sawa, E.; Yamaji, K.; Koezuka, Y.; Kobayashi, E.; Fukushima, H. *J. Med. Chem.* **1995**, *38*, 2176.
- Kawano, T.; Cui, J. Q.; Koezuka, Y.; Toura, I.; Kaneko, Y.; Motoki, K.; Ueno, H.; Nakagawa, R.; Sato, H.; Kondo, E.; Koseki, H.; Taniguchi, M. *Science* **1997**, *278*, 1626.
- Koch, M. R.; Stronge, V. S.; Shepherd, D.; Gadola, S. D.; Mathew, B.; Ritter, G.; Fersht, A. R.; Besra, G. S.; Schmidt, R. R.; Jones, E. Y.; Cerundolo, V. *Nat. Immunol.* **2005**, *6*, 819.
- Borg, N. A.; Wun, K. S.; Kjer-Nielsen, L.; Wilce, M. C.; Pellicci, D. G.; Koh, R.; Besra, G. S.; Bharadwaj, M.; Godfrey, D. I.; McCluskey, J.; Rossjohn, J. *Nature* **2007**, *448*, 44.
- Pellicci, D. G.; Patel, O.; Kjer-Nielsen, L.; Pang, S. S.; Sullivan, L. C.; Kyriakoussis, K.; Brooks, A. G.; Reid, H. H.; Gras, S.; Lucet, I. S.; Koh, R.; Smyth, M. J.; Malleveay, T.; Matsuda, J. L.; Gapin, L.; McCluskey, J.; Godfrey, D. I.; Rossjohn, J. *Immunity* **2009**, *31*, 47.
- Matsuoka, S.; Sugiyama, S.; Matsuoka, D.; Hirose, M.; Lethu, S.; Ano, H.; Hara, T.; Ichihara, O.; Kimura, S. R.; Murakami, S.; Ishida, H.; Mizohata, E.; Inoue, T.; Murata, M. *Angew. Chem., Int. Ed.* **2015**, *54*, 1508.
- Murata, M.; Sugiyama, S.; Matsuoka, S.; Matsumori, N. *Chem. Rec.* **2015**, *15*, 675.
- Hendrickson, W. A.; Rev, Q. *Biophysics* **2014**, *47*, 49.
- Suzuki, T.; Komura, N.; Imamura, A.; Ando, H.; Ishida, H.; Kiso, M. *Tetrahedron Lett.* **2014**, *55*, 1920.
- McDonagh, A. W.; Mahon, M. F.; Murphy, P. V. *Org. Lett.* **2016**, *18*, 552.
- Suzuki, T.; Makyo, H.; Ando, H.; Komura, N.; Menjo, M.; Yamada, Y.; Imamura, A.; Ishida, H.; Wakatsuki, S.; Kato, R.; Kiso, M. *Bioorg. Med. Chem.* **2014**, *22*, 2090.
- Godfrey, D. I.; Kronenberg, M. *J. Clin. Invest.* **2004**, *114*, 1379.
- Matsuda, J. L.; Malleveay, T.; Scott-Browne, J.; Gapin, L. *Curr. Opin. Immunol.* **2008**, *20*, 358.
- Godfrey, D. I.; Rossjohn, J.; McCluskey, J. *Immunity* **2008**, *28*, 304.
- Eberl, G.; MacDonald, H. R. *Eur. J. Immunol.* **2000**, *30*, 985.
- Kawano, T.; Cui, J. Q.; Koezuka, Y.; Toura, I.; Kaneko, Y.; Sato, H.; Kondo, E.; Harada, M.; Koseki, H.; Nakayama, T.; Tanaka, Y.; Taniguchi, M. *Proc. Natl. Acad. Sci. U.S.A.* **1998**, *95*, 5690.
- Carnaud, C.; Lee, D.; Donnars, O.; Park, S. H.; Beavis, A.; Koezuka, Y.; Bendelac, A. *J. Immunol.* **1999**, *163*, 4647.
- Kim, D. H.; Chang, W. S.; Lee, Y. S.; Lee, K. A.; Kim, Y. K.; Kwon, B. S.; Kang, C. Y. *J. Immunol.* **2008**, *180*, 2062.
- Okii, S.; Chiba, A.; Yamamura, T.; Miyake, S. *J. Clin. Invest.* **2004**, *113*, 1631.
- Wilson, S. B.; Delovitch, T. L. *Nat. Rev. Immunol.* **2003**, *3*, 211.
- Bendelac, A.; Savage, P. B.; Teyton, L. *Annu. Rev. Immunol.* **2007**, *25*, 297.
- Brutkiewicz, R. R. *J. Immunol.* **2006**, *177*, 769.
- Nakagawa, R.; Serizawa, I.; Motoki, K.; Sato, M.; Ueno, H.; Iijima, R.; Nakamura, H.; Shimosaka, A.; Koezuka, Y. *Oncol. Res.* **2000**, *12*, 51.
- Duarte, N.; Stenstrom, M.; Campino, S.; Bergman, M. L.; Lundholm, M.; Holmberg, D.; Cardell, S. L. *J. Immunol.* **2004**, *173*, 3112.
- Falcone, M.; Facciotti, F.; Ghidoli, N.; Monti, P.; Olivieri, S.; Zaccagnino, L.; Bonifacio, E.; Casorati, G.; Sanvito, F.; Sarvetnick, N. *J. Immunol.* **2004**, *172*, 5908.
- Hong, S.; Wilson, M. T.; Serizawa, I.; Wu, L.; Singh, N.; Naidenko, O. V.; Miura, T.; Haba, T.; Scherer, D. C.; Wei, J.; Kronenberg, M.; Koezuka, Y.; Van Kaer, L. *Nat. Med.* **2001**, *7*, 1052.
- Hansen, D. S.; Siomos, M. A.; de Koning-Ward, T.; Buckingham, L.; Crabb, B. S.; Schofield, L. *Eur. J. Immunol.* **2003**, *33*, 2588.
- Zeissig, S.; Murata, K.; Sweet, L.; Publicover, J.; Hu, Z.; Kaser, A.; Bosse, E.; Iqbal, J.; Hussain, M. M.; Balschun, K.; Rocken, C.; Arlt, A.; Gunther, R.; Hampe, J.; Schreiber, S.; Baron, J. L.; Moody, D. B.; Liang, T. J.; Blumberg, R. S. *Nat. Med.* **2012**, *18*, 1060.
- Li, X.; Fujio, M.; Imamura, M.; Wu, D.; Vasan, S.; Wong, C. H.; Ho, D. D.; Tsuji, M. *Proc. Natl. Acad. Sci. U.S.A.* **2010**, *107*, 13010.
- Rossjohn, J.; Pellicci, D. G.; Patel, O.; Gapin, L.; Godfrey, D. I. *Nat. Rev. Immunol.* **2012**, *12*, 845.

33. Fuhshuku, K.; Mori, K. *Tetrahedron: Asymmetry* **2007**, *18*, 2104.
34. Fuhshuku, K.; Hongo, N.; Tashiro, T.; Masuda, Y.; Nakagawa, R.; Seino, K.; Taniguchi, M.; Mori, K. *Bioorg. Med. Chem.* **2008**, *16*, 950.
35. Tashiro, T.; Nakagawa, R.; Hirokawa, T.; Inoue, S.; Watarai, H.; Taniguchi, M.; Mori, K. *Tetrahedron Lett.* **2007**, *48*, 3343.
36. Tashiro, T. *Biosci. Biotechnol. Biochem.* **2012**, *76*, 1055.
37. Laurent, X.; Bertin, B.; Renault, N.; Farce, A.; Specca, S.; Milhomme, O.; Millet, R.; Desreumaux, P.; Henon, E.; Chavatte, P. *J. Med. Chem.* **2014**, *57*, 5489.
38. Zajonc, D. M.; Cantu, C.; Mattner, J.; Zhou, D. P.; Savage, P. B.; Bendelac, A.; Wilson, I. A.; Teyton, L. *Nat. Immunol.* **2005**, *6*, 810.
39. Lee, T.; Cho, M.; Ko, S. Y.; Youn, H. J.; Baek, D. J.; Cho, W. J.; Kang, C. Y.; Kim, S. *J. Med. Chem.* **2007**, *50*, 585.
40. Lim, C.; Kim, J. H.; Baek, D. J.; Lee, J. Y.; Cho, M.; Lee, Y. S.; Kang, C. Y.; Chung, D. H.; Cho, W. J.; Kim, S. *ACS Med. Chem. Lett.* **2014**, *5*, 331.
41. Miyamoto, K.; Miyake, S.; Yamamura, T. *Nature* **2001**, *413*, 531.
42. Henon, E.; Dauchez, M.; Haudrechy, A.; Banchet, A. *Tetrahedron* **2008**, *64*, 9480.
43. Fujio, M.; Wu, D. G.; Garcia-Navarro, R.; Ho, D. D.; Tsuji, M.; Wong, C. H. *J. Am. Chem. Soc.* **2006**, *128*, 9022.
44. He, W. G.; Soll, C. E.; Chavadi, S. S.; Zhang, G. T.; Warren, J. D.; Quadri, L. E. N. *J. Am. Chem. Soc.* **2009**, *131*, 16744.
45. Takaya, Y.; Kikuchi, H.; Terui, Y.; Komiya, J.; Furukawa, K. I.; Seya, K.; Motomura, S.; Ito, A.; Oshima, Y. *J. Org. Chem.* **2000**, *65*, 985.
46. Golmohammadi, R. *Ark Kemi* **1966**, *25*, 279.
47. Tong, Y.; Deacon, M. L.; Zelakiewicz, B. S. *Synlett* **2005**, 1618.
48. Hancock, A. N.; Lobachevsky, S.; Haworth, N. L.; Coote, M. L.; Schiesser, C. H. *Org. Biomol. Chem.* **2015**, *13*, 2310.
49. Schwarz, K.; Fredga, A. *Bioinorg. Chem.* **1975**, *4*, 235.
50. Ding, N.; Li, C. X.; Liu, Y. P.; Zhang, Z. H.; Li, Y. X. *Carbohydr. Res.* **2007**, *342*, 2003.
51. Crich, D.; de la Mora, M.; Vinod, A. U. *J. Org. Chem.* **2003**, *68*, 8142.
52. Xia, C.; Schumann, J.; Emmanuel, R.; Zhang, Y.; Chen, W.; Zhang, W.; De Libero, G.; Wang, P. G. *J. Med. Chem.* **2007**, *50*, 3489.
53. Pal, E.; Tabira, T.; Kawano, T.; Taniguchi, M.; Miyake, S.; Yamamura, T. *J. Immunol.* **2001**, *166*, 662.
54. Hsieh, M. H.; Hung, J. T.; Liw, Y. W.; Lu, Y. J.; Wong, C. H.; Yu, A. L.; Liang, P. H. *Chembiochem* **2012**, *13*, 1689.
55. Liang, P. H.; Imamura, M.; Li, X.; Wu, D.; Fujio, M.; Guy, R. T.; Wu, B. C.; Tsuji, M.; Wong, C. H. *J. Am. Chem. Soc.* **2008**, *130*, 12348.
56. Schiefner, A.; Fujio, M.; Wu, D.; Wong, C. H.; Wilson, I. A. *J. Mol. Biol.* **2009**, *394*, 71.